https://doi.org/10.33261/jaaru.2020.27.1.003 *Association of Arab Universities Journal of Engineering Sciences (2020) 27(1): 19–29*

Association of Arab Universities Journal of Engineering Sciences

مجلة اتحاد الجامعات العربية للدراسات والبحوث الهندسية

Extended Finite Element Analysis of Reinforced Concrete Beams Using Meso-Scale Modeling

***Eman Abbas*[1], and *Alaa H. Al-zuhairi*[2, *]**

[1]*University of Baghdad – College of Engineering, Al-Jadriya, Baghdad, Iraq, E-mail: dremancivil2019@gmail.com*

[2] *University of Baghdad – College of Engineering, Al-Jadriya, Baghdad, Iraq, E-mail: alaalwn@coeng.uobaghdad.edu.iq*

*Eman Abbas *dremancivil2019@gmail.com*

Published online: 31 March 2020

Abstract— Four simply supported reinforced concrete (RC) beams were test experimentaly and analyzed using the extended finite element method (XFEM). This method is used to treat the discontinuities resulting from the fracture process and crack propagation in that occur in concrete. The Meso-Scale Approach (MSA) used to model concrete as a heterogenous material consists of a three-phasic material (coarse aggregate, mortar, and air voids in the cement paste). The coarse aggregate that was used in the casting of these beams rounded and crashed aggregate shape with maximum size of 20 mm. The compressive strength used in these beams is equal to 17 MPa and 34 MPa, respectively. These RC beams are designed to fail due to flexure when subjected to load as a two-point loading. To model the coarse aggregate realistically, the aggregate must distributed randomly according to the gradient and amount actually used in the mix design. This property is not found in the ABAQUS program that resulted in the use of an alternate program to represent the aggregate randomly. Next, the random representation of the aggregate were transfered to the ABAQUS program by using commands and instructions that the program can understand, to draw as a sketch. The comparison between experimental and numerical results showed that the XFEM is a good method used to simulate the non-smooth behavior in RC beams such as discontinuitiy and singularity. While a mesoscale model can be simulated the non-homogeneity in the concrete.

Keywords— Extended Finite Element Method, fracture mechanics, Mesoscale modeling, crack propagation.

1. Introduction

The term concrete refers to a mixture of aggregates, sand, gravel or crushed stone, and air voids in the cement paste held together by a binder of cementations paste.

Many studies used different small scales in the analysis of concrete such as meso-, micro-, and even nano scales to understand the behavior of the composite materials and to reach, approximately, the failure point of the material [3], [9-11], and [17]. In this study, the meso scale model will be used to concrete modeling.

In this paper, RC simply supported beam subjected to flexural stresses was tested in the laboratory. The same types of beams were analyzed numerically using the meso scale model. Flexural stresses were produced by a two-point loading system. The XFEM was used for treatment of the discontinuity problem.

2. Meso-Scale Modeling

Generally, meso scale means “middle scale” or “in-between scale”. This falls between the macro- and micro scales. Since the mid-1980s, many meso scale models for concrete have made their appearance. The main advantage of these models over classic constitutive models for concrete is their ability to simulate material heterogeneity, and its effect on damage evolution and fracture.

The meso scale modeling can be classified into two types:

1. The continuum models.
2. The lattice models.

In the continuum models, concrete is modeled as a continuum composite material which consists of aggregate, mortar, and interface between the two materials [13]. In the lattice models, concrete is modeled as a discrete system consisting of a lattice element [15]. In the lattice modeling method, require a huge numerical effort to obtain the concrete meso structure that will be accepted for the analysis. In this study, a continuum mesoscale model was used to model the concrete.

The meso scale, for heterogeneous materials like concrete, might be modeled with two or three different phases at least. In this study, a meso scale model in concrete can be treated as a three-phase composite material consisting of cement mortar, aggregates, and air voids in the cement paste. The contact area that interfaces both mortar and aggregates will be modelled as fully bonded and tied with the concrete that makes the two materials, is assumed to be fully consistent.

The modeling of concrete in meso scale has two approaches:

a. The image-based modeling, and
b. The parameterization modeling.

3. The Discontinuities and Singularities

Discontinuities are generally divided into two categories; strong and weak discontinuities, as shown in Figure 1, [12] and [14].

Strong discontinuity is the discontinuity in the solution variable of a problem, that is, the displacements in structural problem. So, displacement jumps like cracks and holes are considered as strong discontinuities. In this category of discontinuities, the interface is referred to as open interface where it cuts the domain partially so that at least one end of the interface is inside the domain. A good example of such discontinuity is the cracked domain.

Weak discontinuities are those found in the derivatives of the solution variable. In structures, such discontinuities would involve kinks in the displacements i.e., a jump in the strains, for example, the bimaterial problems. In these types of discontinuities, the interface is called closed interface that links different materials in the domain see Figure 1.

The fractured domain causes a singularity in the stress field at the crack tip region.

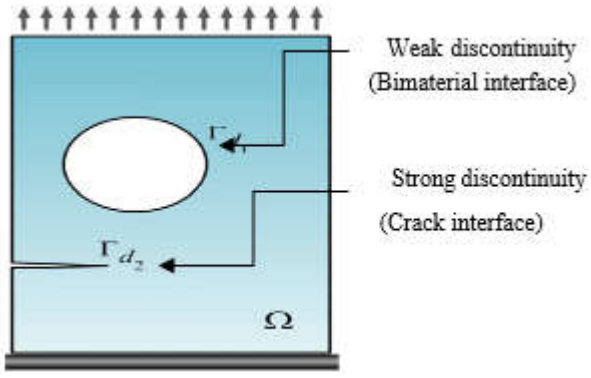

Figure 1: Weak and strong discontinuities [12].

4. The Extended Finite Element /method (XFEM)

Many techniques were developed to solve the problems on the basis of fracture mechanics analysis, discontinuities and singularity problems such as:

1. The remeshing technique used for the crack modeling [20].

2. The element detection method for the simulation of crack development and propagation [5].

3. The smeared cracking method which is used for the analysis of concrete cracking, and was introduced by [16].

4. Interelement separation method [23], and [8].

5. Enrichment method [6].

- A .The XFEM is an enrichment method utilized for the discontinuities problems, which was developed by [7].
- The Generalized Finite Element Method (GFEM) is an enrichment method which was developed by [19].

Modeling of crack propagation with the FEM is needed to update the mesh to conform to the geometry of the crack surface. Several FE techniques have been developed to model cracks and crack growth without remeshing. The enrichment method is used for solving problems with discontinuities, singularities, and many other complex problems that cannot be solved by the FEM.

The XFEM and the GFEM are useful tools for this problem. The differences between the XFEM and GFEM are that the XFEM uses local enrichment methods, while the GFEM utilized global enrichment methods; on the other hand, the GFEM permits the p-adaptivity with an accurate solution for the modeled mesh, while the XFEM interest with the enrichment of nodes is needed for the solution of discontinuities such as cracks and interfaces.

This study used the X-FEM to solve the problem of discontinuities.

The Extended Finite Element Method (XFEM) is a numerical method, designed for treating discontinuities and singularities in the material. This technique used to model weak and strong discontinuities without considering their geometries [12]. In the XFEM, special functions are added to the finite element approximation using the framework of the partition of unity (PU). The mathematical background of XFEM is the partition-of-unity concept. The concept of PU can be used to provide a mathematical framework for the development of an enriched solution. The PUM is used to enhance the approximation by adding the enrichment functions to the standard approximation.

The XFEM method is based on adding the enrichment terms to the standard or regular interpolation of the approximation field, and is as shown in Equation 1

$$u(x) = \sum_{i=1}^{N} N_i(x) \times \bar{u}_i + enrichment\ terms \quad \ldots\ldots 1$$

$$u(x) = \underbrace{\sum_{i=1}^{N} N_i(x) \times \bar{u}_i}_{\text{regular interpolation}} + \underbrace{\sum_{k=1}^{p} \bar{N}_i(x) \times \left(\sum_{j=1}^{M} \psi_j(x) \times \bar{a}_{ij}\right)}_{\text{enrichment interpolation}} \quad \ldots\ldots 2$$

Where

$\bar{a}_i$: enrichment DOF

M: the number of enrichment nodes

$\psi_j(x)$: the enrichment function.

p: the number of enrichment functions.

5. The Enrichment of Approximation Field

The enrichment is an act of improving the approximation of discretization based on the properties of the problem. The enrichment increases the accuracy of the approximation by including information of the analytical solution. The enrichment of approximation space is one of the most efficient techniques that can be used to capture the weak or strong discontinuities. [12]. There are two ways of enriching an approximation field: intrinsic and extrinsic enrichments. The extrinsic enrichment is based on the PU concept. In this method, the enrichment functions are added to the standard approximation. The enrichment varies from element to element, where some element requires partial enrichment (blending elements where, in this enrichment, some of the nodes are enriched), while some element requires full enrichment, and many elements require no enrichment.

Different techniques may be used for the enrichment function; these functions are related to the type of discontinuity and its influences on the form of the solution. These techniques are such as the signed distance function, level set function, the near-tip asymptotic functions, branch functions, Heaviside jump function, and so on. The choice of enrichment functions in displacement approximation is dependent on the conditions of the problem [12].

6. The Enrichment Functions

For weak discontinuity (the discontinuity results from differences in the type of material properties), the level set function was used as an enrichment function (see Equation 3).

$$u_{weak\ discontinuity}(x) = \sum_{i=1}^{N} N_i(x) \times \bar{u}_i + \sum_{j=1}^{M} N_j(x) \times (|\varphi(x)| - |\varphi(x_j)|) \times \bar{a}_j \quad \ldots\ldots 3$$

$$\varphi(\vec{x}) = \vec{N}\, d(\vec{x}) \quad \ldots\ldots 4$$

$$\varphi(x) = \begin{cases} > 0\ if\ \vec{x} \in \Omega A \\ 0\ \text{if}\ \vec{x} \in \Gamma \text{d} \\ < 0\ \text{if}\ \vec{x} \in \Omega \text{B} \end{cases} \quad \ldots\ldots 5$$

Where

$\varphi(\vec{x})$: is the signed distance to the closest point on the interface, (see Figure 2)

$\vec{\text{N}}$: is the local unit normal at$\vec{x}$ takes the value (+ or -) that referred to outside region and inside region. Then $\varphi(\vec{x})$ can be written as shown in Equation 6

$$\varphi(x) = d(x)\ sign\left(n_{\Gamma \text{d}}(x - x_c)\right) = |x - x_c| sign\left(n_{\Gamma \text{d}}(x - x_c)\right) \quad \ldots\ldots 6$$
$$sign\left(n_{\Gamma \text{d}}(x - x_c)\right) = \vec{N}$$

Where

$n_{\Gamma \text{d}}$: is the normal vector to the interface at point x_c.

For strong discontinuity (the discontinuity results from crack) two types of enrichment functions are used: Heaviside or step function (jump function), and asymptotic near-tip enrichment function [12]. The Heaviside function is one of the most popular enrichment functions used to model the crack discontinuity in the XFE formulation when cracks cut the elements and split the domains into two parts. In case the element contains the crack tip, then part of the element is cut and part of it is not, hence, in these cases, the step function cannot be used to enrich the domain where step function or a Heaviside enrichment is good when the element is totally cut by the crack, such that it divides the element into two. In such a case, the asymptotic near-tip enrichment function was used.

$$u_{crack}(x) = \sum_{i\in N} N_i(x) \times \bar{u}_i + \sum_{j\in N^{dis}} N_i(x) \sum_{j=1}^{M} N_j(x) \times \left(H(x) - H(x_j)\right) \times \bar{d}_j + \sum_{k\in N^{tip}} N_k(x) \times \sum_{a=1}^{4} (B_a(x) - B_a(x_k)) \times \bar{b}_{ak} \quad (7)$$

Where:

N^{dis} : The set of enriched nodes whose support is bisected by the crack

N^{tip}: The set of nodes which contains the crack tip in the support of their shape functions enriched by the asymptotic functions

$\bar{u}_i$: The unknown standard nodal DOF at I^{th}node

$\bar{d}_j$: The unknown enriched nodal DOF associated with the Heaviside enrichment function at node J

$\bar{b}_{ak}$: The additional enriched nodal DOF associated with the asymptotic functions at node K.

7. Experimental Work

Four RC beams with minimum reinforcement casting were subjected to testing in the laboratory, which yields into 2 Ø 8 mm top bars and 2 Ø 12 mm bottom bars. Shear reinforcement was also used by Ø 8 mm stirrups distributed along the entire length of the beam with 150 mm c⁄c spacing (see Figure 2). The rounded coarse aggregate with maximum size of 20 mm was used to cast these beams. The coding procedure of the RC beams used in this study is illustrated below:Coding example: a-M b-c

Where;

a: denote the compressive strength of concrete in Mpa.

b: denote the maximum size of coarse aggregate in mm.

c: denote the type of the coarse aggregate used (crushed, or rounded).The RC beams having the different compressive strength and differ in the shape of the coarse aggregate particles as shown in Table 1.

Table 1: RC beams details.

Compressive Strength, MPa	Aggregate Type	Beam Code No.
17	Rounded Aggregate	17-M 20- R
	Crushed Aggregate	17-M 20- C
34	Rounded Aggregate	34-M 20- R
	Crushed Aggregate	34-M 20- C

These beams were designed to fail in flexure. The dimensions of the beams were 2400 × 350 × 200 mm, with different compressive strengths of 17 MPa and 34 MPa. These beams were tested under two-point loads (see Figure 3). The RC beams were notched at the midspan length of each beam on the bottom face for crack initiation. The amounts of the material used in casting these beams are explained in Table 2, and were designed and executed according to [1].

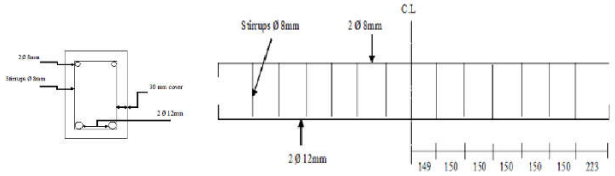

Figure 2: Section in the beam model.

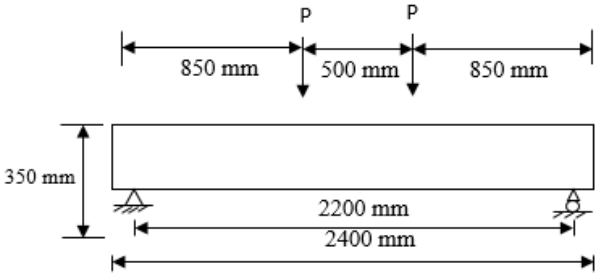

Figure 3: Reinforced concrete beam model.

Table 2: Design mix proportions for the concrete beam specimens

Beam Code No	RCB1	RCB2
Cement kg/m^3	273	424
Coarse aggregate kg/m^3	1180	1180
Fine aggregate kg/m^3	621	494
Mixing water kg/m^3	205	205
Air voids content %	2	2

Five electric strain gauges were attached to each RC beam specimen. One of these gauges was attached at the middle of the front face of the specimens in the tension zone. Another gauge was attached at the middle of the bottom face of the specimens. These two strain gages were used to measure the tensile strain at midspan of the RC beam specimens (see Figure 4). The other three strain gages were attached at the shear zone at a distance equal to d / 2 from the support. These strain gages were attached so that they formed a rosette strain gage which was used to measure the shear strains (see Figure 5). The strain gauges were linked to the electronic strain reader (data logger). The data logger and strain gauges were calibrated according to ASTM E 251-92, [4]. Dial gauges were used for deflection measurements where they were located at midspan of the bottom face of the RC beam specimens.

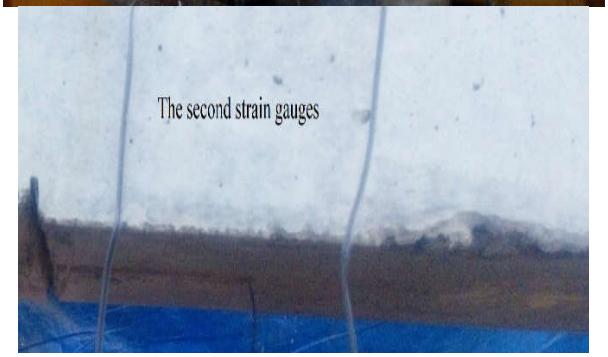

Figure 4: Strain gauges measured the tensile strain at midspan of the RC beam specimens.

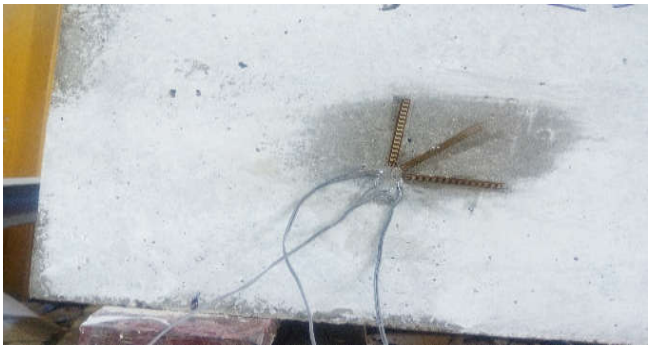

Figure 5: Rosette strain gauge.

8. Numerical Work

In this study, different shape of coarse aggregate, grading and different compressive strengths were used. As mentioned earlier, another program was used in the modeling of coarse aggregate and air voids. EXCEL sheets were used for calculations and drawing of the quantity of the coarse aggregate for the two-dimensional area (2D) of the beams and were computed from the mix design of the concrete [2]. It will be needed to make EXCEL sheets for each gradient. Also, it is required to find the area of coarse aggregate required in each gradient. Table 3 and 4 explains the area of aggregate required in each gradient for round and crashed coarse aggregate. The content of the air voids was assumed equal to the theoretical percentages given in [1] for the design mix properties.

Table 3: area of round aggregate for each gradient to maximum size 20.

Sieve size, mm	Specified required passing % according to ASTM C33	Passing %	Return at each seive %	Area for each gradient $\boldsymbol{mm^2}$ ($\boldsymbol{\text{Return}}$ % × $\boldsymbol{CA_{area}}$)
19.00	100	100	0	0
9.50	40 to 70	45.72	54.28	189980
4.75	0 to 15	0.76	44.96	157360
2.36	0 to 5	0	0.76	2660
1.18	≈0	0	0	0

Table 4: area of crashed aggregate for each gradient to maximum size 20.

Sieve Size, mm	Specified required Passing % according to ASTM C33	Passing %	Return at each seive %	Area for each gradient $\boldsymbol{mm^2}$ ($\boldsymbol{\text{Return}}$ % × $\boldsymbol{CA_{area}}$)
19.00	100	100	0	0
9.50	40 to 70	67	33	108900
4.75	0 to 15	0.3	66.7	220110
2.36	0 to 5	0.04	0.26	858
1.18	≈0	0	0	0

In this study, rounded and crushed coarse aggregate will be used. Placement of aggregate particles in their positions should be done with the following conditions:

1. All aggregate particles should be located inside the concrete area. This condition is treated by using a text file written using the PYTHON file format then imported to ABAQUS.
2. Aggregate particles were separated by a minimum distance of (0-1) mm.
3. Aggregate particles should be partly away from the edges of the concrete beam by not less than 2.5 mm [18].

The round coarse aggregate particles and air voids are assumed as elliptical shapes. To draw an elliptical shape it is required to randomly calculate the following parameters:

1. Centre coordinates (x,y)
2. The major radius (a)
3. The minor radius (b)
4. Two-point at the circumference of the ellipse (P_1 and P_2) (see Figure 6)
5. The orientation of particle (θ)
6. The points of the ellipse after being rotated about the center $\overline{P_1}$ and $\overline{P_2}$(see Figure 6)
7. Area of the particle
8. Accumulated area

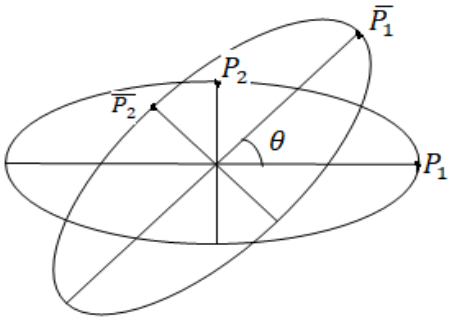

Figure 6: An ellipse point rotating about the center.

To model the crushed aggregate as a polygon in EXCEL sheets it is needed to take into account some points.

1. The center of the polygon (x,y)
2. The effective diameter of the aggregate (D) is calculated randomly between any two sieve confining between them, (the value is limited between the maximum and minimum value of sieve opining)
3. Find the radius of the aggregate (R), R=D⁄2
4. Select polygon key points . The key points that needed to be determined depend on the number of the polygon sides. The center and radius are defined to draw a point on distance R from the center. In addition it is required to define the angle of the ribs from x –axis. The angle takes counter clockwise from x –axis. For example to draw a polygon have six sides it is needed to select six points; the first point located at the first quarter, the second point located at the second quarter, the third point located at the third quarter, the fourth point located at the fourth quarter, the fifth point located at the first quarter and the sixth point located at the second quarter.

The angle (θ_i) is calculated in radian using the following order:

To find the polygon key points it is required to find the coordinate of each point p_i (x_i, y_i)

$$x_i = x + R\cos\theta_i \quad (8)$$

$$y_i = y + R\sin\theta_i \quad (9)$$

The above equations are used as a general concept. In this order input (if - else condition) to arrange the point when find two points in the same quarter. For example polygon have 5 points in this case point 1 and 5 lies in the first quarter, then to calculate x_1 , y_1 use:

if $\theta_1 < \theta_5$ then $x_1 = x + R\cos\theta_1$ else $x_1 = x + R\cos\theta_5$

if $\theta_1 < \theta_5$ then $y_1 = y + R\sin\theta_1$ else $y_1 = y + R\sin\theta_5$

To calculate x_5 , y_5

if $\theta_1 > \theta_5$ then $x_5 = x + \cos\theta_1 \times R$ else $x_5 = x + R\cos\theta_5$

if $\theta_1 > \theta_5$ then $y_5 = y + \sin\theta_1 \times R$ else $y_5 = y + \sin\theta_5 \times R$

The above order are used to find two points in the same quarter.

5. Calculate the area of the polygon

$$\text{Area of polygon (A)} = \frac{1}{2}\left|\left[\sum_{i=0}^{n-1}(x_i \times y_{i+1}) - \sum_{i=0}^{n-1}(x_{i+1} \times y_i)\right] + \left[(x_n \times y_1) - (y_n \times x_1)\right]\right| \quad (10)$$

Then find the cumulative area to get the same amount of aggregate required to be provided between the two sieves.

The coordinate of the polygon points were determined using orders in EXCEL sheet.

To draw the polygon, the key points should be connected by lines. For this purpose Auto CAD program is used.

PL : is the polygon line (order used in Auto CAD program to draw lines between points). This order is used to draw the crushed aggregate directly in Auto CAD program. Then the sketch is saved as DXF file and the ABAQUS program will import this sketch from Auto CAD program.

In the numerical analysis, the properties of the cement mortar and the aggregate particles were selected according to [22] [see Table 5]. The air voids were assumed as space voids in the concrete model without any material properties.

Table 5: Materials and their properties used in the ABAQUS program.

Material	Modulus of Elasticity MPa	Poisson's Ratio	Fracture Energy N-mm/mm^2
Aggregate	75000	0.2	-
Mortar	25000	0.2	0.06
Steel	200000	0.3	-

In the ABAQUS program a programing PYTHON language was used for RC beams modeling.

The model is defined the ABAQUS program as a sketch with name of rectangular have the same dimension of the beams in 2D in this sketch insert the cumulative coarse aggregate area for each gradients.

9. Results and discussion

The RC beams were tested in two-point loading cases. Table 4 shows the experimental and numerical maximum applied loads on the RC beams till failure.

Table 6: Results of maximum applied load.

Beam Code No.	Maximum applied load (kN) in experimental work	Maximum applied load (kN) in numerical analysis
17-M 20- R	81.5	110
34-M 20- R	104	120
17-M 20- C	84.6	91.4
34-M 20- C	108	113

From Table (4), it can be noted that the beams of compressive strength 34 Mpa are stronger than the other one. Figure 7 and 8 shows the load-deflection curve experimentally measured and numerically determined at midspan of the RC beams constructed using rounded and crushed coarse aggregate of maximum size 20 mm for two different compressive strengths of 17 Mpa and 34 Mpa respectively.

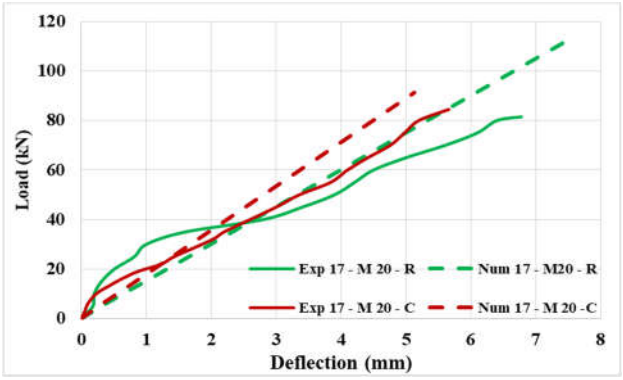

Figure 7: Load – deflection curves for RC beams have compressive strength 17 MPa.

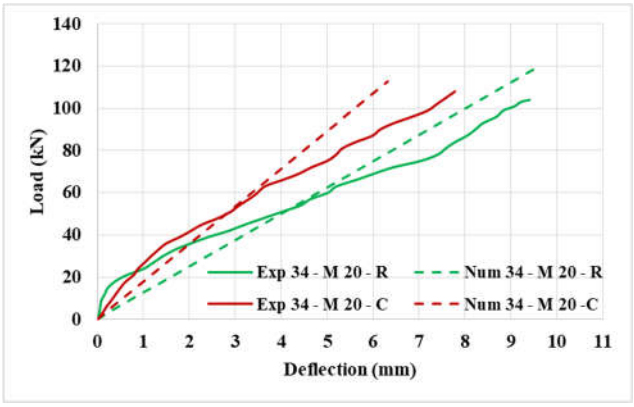

Figur 8: Load – deflection curves for RC beams have compressive strength 34 MPa.

From the above figures, the load deflection curves for RC beams are convergent for numerical and experimental curve for beams constructed using different coarse aggregate shape (round and course) that have the same maximum size 20mm.

Using crashed coarse aggregate (angular particles) led to decrease the deflection when compared with beams have the same maximum size and at the same load. On the other hand, increasing the strength of the concrete beam result in a decrease of the mid span deflection. When the compressive strength increases, the maximum deflection will be increased because the maximum applied load is greater than the other one.

The relation between the applied loads for experimentally and numerically measured tensile strain at midspan of the RC beams of rounded and crushed coarse aggregate of maximum size 20 mm for two different compressive strengths of 17 Mpa and 34 Mpa respectively are shown in Figure 9 and 10.

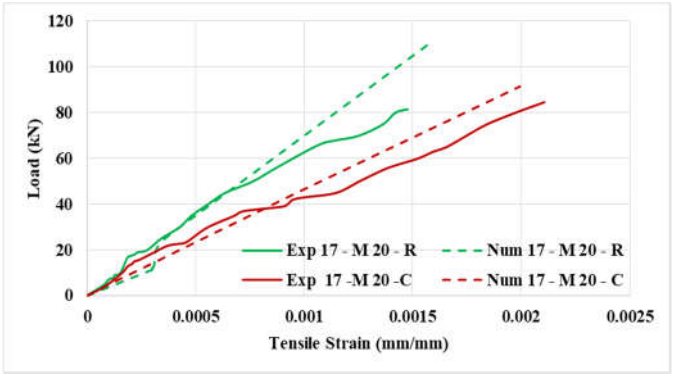

Figure 9: Load – tensile strain curves for RC beams have compressive strength 17 MPa.

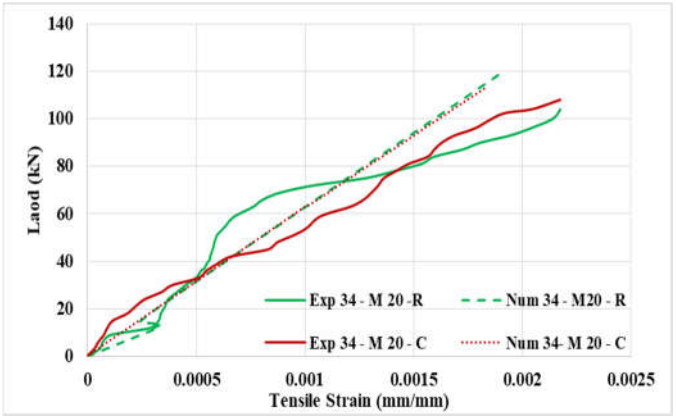

Figure 10: Load – tensile strain curves for RC beams have compressive strength 34 MPa.

From above figures when the compressive strength increases to 34 MPa the experimental curves of tensile strain become more convergence for RC beams have the same maximum size and different coarse aggregate shape. In the numerical analysis the convergence of numerical results is increased with increasing the compressive strength. For example in Figure 9. when the compressive

strength equal to 17 Mpa the behavior of beams 17 M 20 R and 17 M 20 C are close to each other. While in Figure 10. the numerical results are identical for 34 M 20 R and 34 M 20 C beams. However, when the compressive strength is increased the type of aggregate (round or crashed) becomes in efficient to the amount of the tensile strain.

As shown in the above figures, the load-tensile strain curves of the numerical analysis for RC beams show a snap-back phenomena although the numerical analysis was done in terms of linear elastic fracture mechanics.

From the above, the experimental and numerical curves are approximately similar to each other. From this, the numerical results get a good agreement from analysis of the model numerically when using the program to obtain good agreement and approximation with the experimental result

The load-shear strain curves for the numerical and experimental data are shown in Figure 11 and 12 for rounded and crushed coarse aggregate with maximum size of 20 mm that have a compressive strength equal to 17 MPa and 34 MPa, respectively.

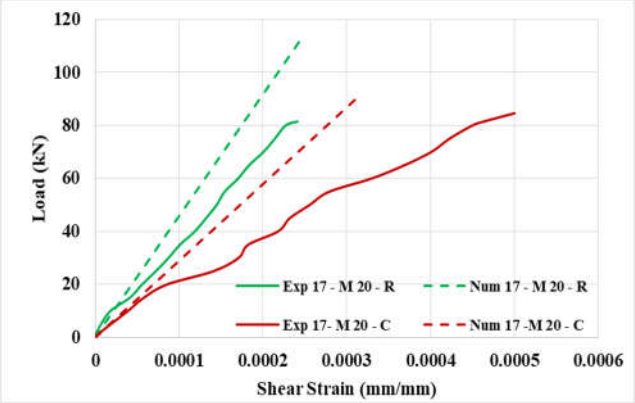

Figure 11: Load – shear strain curves for RC beams have compressive strength 17 MPa.

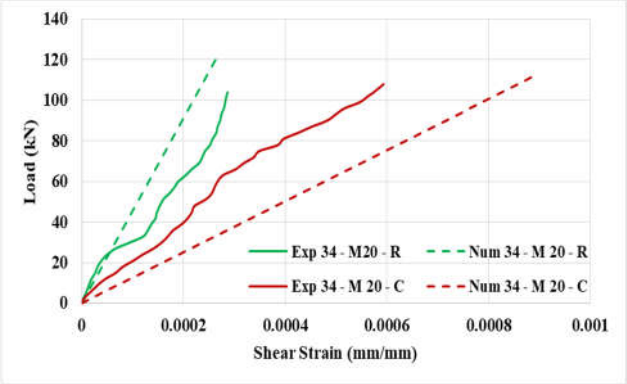

Figure 12: Load – shear strain curves for RC beams have compressive strength 34 MPa.

As shown in this figure, the numerical shear strains behave linearly with the increasing of the applied load. From the above figures it can be see that the beams have round coarse aggregate sustain shear strain leas than beams have crushed coarse aggregate. Also, it can be observed that the beams of crushed coarse aggregate have somewhat different behavior when compared with beams of rounded coarse aggregate. In addition the measured shear strains were found in beams of crushed coarse aggregate greater than those measured in the beams of rounded coarse aggregate this is may be attributed to the effect of interlock of crushed coarse aggregate.

The bending stress distribution along the beam midspan section for the numerical analysis are shown in Figure 13.

As can be seen from the previous figure, the distribution of the bending stresses along the beam section is not constant. Where the stresses take negative values at the top of the RC beam, positive values are taken at the bottom. Near the centre of the beam the stresses become zero.

From the above figure, it can be noted that stress values are high because of a non-homogeneity of the concrete material, and assuming the interface to be a fully bonded interface (tie). The coarse aggregate particles and air voids at the section of the beam causes stress concentration problems. In addition, assuming a connectivity between the coarse aggregate, cement mortar and air voids as fully bonded, and that make the location of the interface as supported, this leads to stress concentration problems, as can be seen in the above figures.

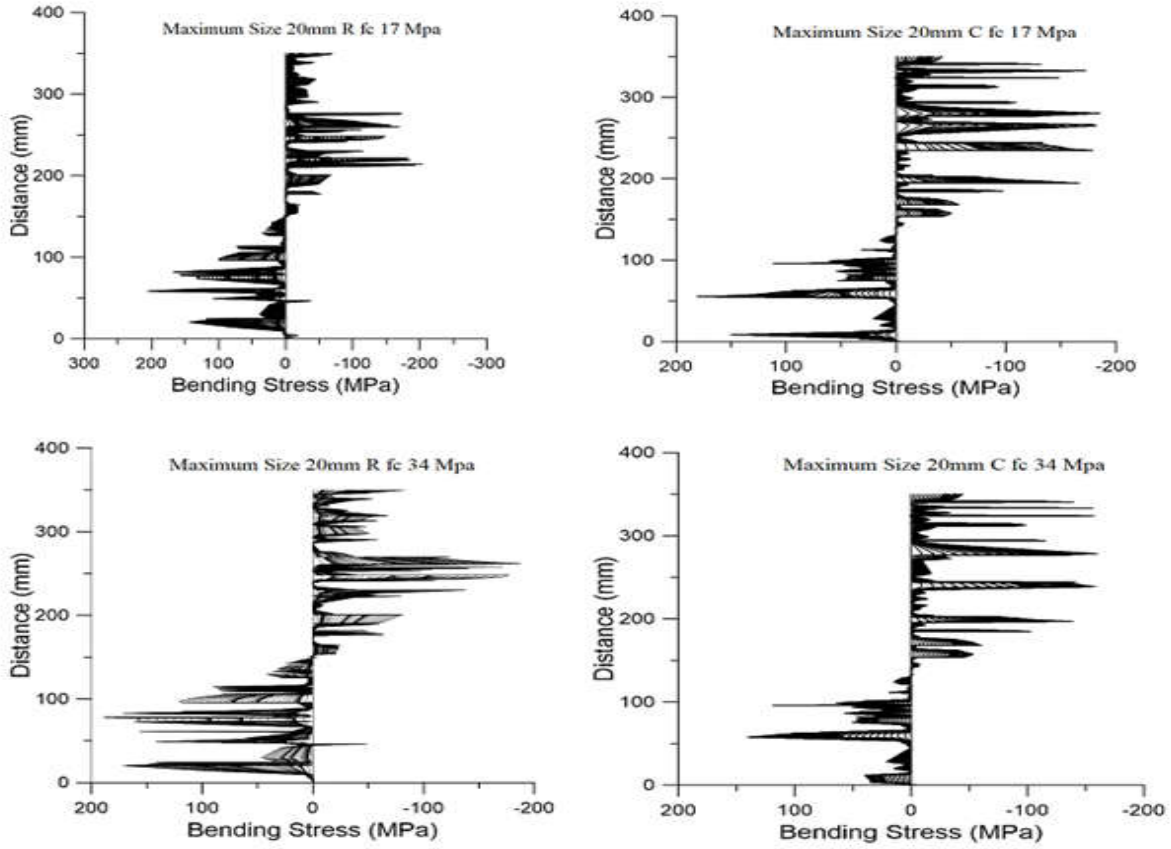

Figure 13: Bending stress distribution for RC beams.

10. Conclusions

1. XFEM is a powerful method used to treat the discontinuities resulting from the fracture process and crack propagation in concrete and singularity in the stress field at the crack tip region.

2. The numerical analysis for the deflection of the mesoscale model gave about more than 88% convergence with the experimental data.

3. The comparison between the numerical analysis and experimental work for the tensile strain behavior gave about more than 90% convergence.

4. A non-homogeneity of the concrete material, the coarse aggregate particles and air voids at the section of the beam causes stress concentration problems.

5. Assuming the interface between the coarse aggregate, cement mortar and air voids as a fully interface-bonded tie, gave higher values of bending stress.

6. A mesoscale FE model was used for random concrete particles modeling. It was found to be a good approach for representing the non-homogeneity of the concrete.

References

[1] ACI 211-02. “Standard practice for selecting properties for normal, heavyweight, and mass concrete. American Concrete Institute, ACI. (2002).

[2] Al-Zuhairi, A. H., and A. I. Taj “Finite element analysis of concrete beam under flexural stresses using meso-scale model”. Civil Engineering Journal, Vol. 4, no. 6, pp. 1288-1302, June, 2018.

[3] Al-Zuhairi, A. H., and A. I. Taj. “Effectiveness of Meso-Scale Approach in Modeling of Plain Concrete Beam”, Journal of Engineering, Vol. 24, no.8, pp. 71-80, July, 2018.

[4] ASTM E251-92. “Standard test method for performance characteristics of metallic bond resistance strain gages”. American Society for Testing and Materials, 1992.

[5] Beissel, S. R., Johnson, G. R., & Popelar, C. H., "An element failure algorithm for dynamic crack propagation in general directions." Engineering

Fracture Mechanics, Vol. 61, no. (3-4), pp.407-425, 1998.

[6] Belytschko, T., Fish, J., Engelmann, B.E., "A finite element with embedded localization zones", Computer Methods in Applied Mechanics and Engineering, Vol. 70, pp. 59–89, 1988.

[7] Belytschko, T. and Black, T., "Elastic crack growth in finite elements with minimal remeshing". International Journal for Numerical Methods in Engineering, Vol. 45, pp. 601–620, 1999.

[8] Camacho GT, Ortiz M., "Computational modeling of impact damage in brittle materials". International Journal of Solids Structures, Vol. 33, no. (20-22), pp. 2899–2938, 1996.

[9] Carpinteri, A., and P. Cornetti., "A multiscale approach to concrete fracture: the influence of the aggregate grading", In Convegno IGF XVI Catania, 2002.

[10] Eftekhari, M., S. H. Ardakani, and S. Mohammadi, "An XFEM multiscale approach for fracture analysis of carbon nanotube." Theoretical and Applies Fracture Mechanics, Vol. 72, pp. 64-75, 2014.

[11] Huang, J., Chen, M., & Sun, J., "Mesoscopic characterization and modeling of microcracking in cementitious materials by the extended finite element method." Theoretical and Apllied Mechanics letters, Vol. 4, no. 4, pp. 041001, 2014.

[12] Khoei A.R., Extended Finite Element Method Theory and Application. Sharif University of Technology, Iran, 2015.

[13] Liao, K.Y., Chang, P.K., Peng, Y.N. and Yang, C.C., "A study on characteristics of interfacial transition zone in concrete". Cement and Concrete Research, Vol. 34, no. 6, pp.977-989, 2004.

[14] Mohammadi., S., "Extended Finite Element Method for Fracture Analysis of Structures", Blackwell Publishing, 2008.

[15] Nitka, M. and Tejchman, J., "Modelling of concrete behaviour in uniaxial compression and tension with DEM". Granular Matter, Vol. 17, no. 1, pp.145-164, Feb, 2015.

[16] Rashid, Y. R., "Analysis of Prestressed Concrete Pressure Vessels". Nuclear Engng. and Des., Vol. 7, no. 4, pp. 334-355, 1968.

[17] Roubin, E., Colliat, J. B., & Benkemoun, N., "Meso-scale modeling of concrete: a morphological description based on excursion sets of Random Fields." Computational Materials Science, Vol. 22, no. 102, pp. 183-195, Feb., 2015.

[18] Shahbazi, Siamak, and Iraj Rasoolan. "Meso-Scale Finite Element Modeling of Non-Homogeneous Three-Phase Concrete." Case Studies in Construction Materials, Vol. 6, pp. 29–42, June, 2017.

[19] Strouboulis, T., K. Copps, and I. Babuska., "The generalized finite element method: an example of its implementation and illustration of its performance." International Journal for Numerical Methods in Engineering, Vol. 47, pp. 1401-1417, 2002.

[20] Swenson, D. V., & Ingraffea, A. R., "Modeling mixed-mode dynamic crack propagation nsing finite elements: Theory and applications." Computational Mechanics, Vol. 3, no. 6, pp.381-397, September, 1988.

[21] Sylvie Pommier, John Wiley and Sons, "Extended Finite Element Method for Crack Propagation", 2011.

[22] Wang, X., Yang, Z., Yates, J., jivkov, A., and Zhang, "Monte Carlo Simulations of meso scale fracture modeling of concrete with random aggregate and pores", Construction and Building Materials, Vol. 75, PP. 35-45, 2015.

[23] Xu XP, Needleman A., "Numerical simulations of fast crack growth in brittle solids". Journal of the Mechanics and Physics of Solids, Vol. 42, pp. 1397–1434, 1994.

تحليل العناصر الممتدة المحدودة للعوارض الخرسانية المسلحة باستخدام نمذجة النطاق المتوسط

***ايمان عباس*[1]، علاء *حسين علوان*[2] ***

[1] *جامعة بغداد، كلية الهندسة، بغداد، العراق، dremancivil2019@gmail.com*

[2] *جامعة بغداد، كلية الهندسة، بغداد، العراق، alaalwn@coeng.uobaghdad.edu.iq*

* *ايمان عباس، dremancivil2019@gmail.com*

نشر في: 31 آذار 2020

الخلاصة – تم تحليل اربع اعتاب خرسانية مسلحة (RC) ومسندة أسناد بسيطا (Simply Supported) بأستخدام طريقة العناصر المحددة الممتدة (XFEM). تستخدم هذه الطريقة لعلاج حالات عدم الاستمرارية الناتجة من عملية الكسر وانتشار الشقوق في الخرسانة. يستخدم طريقه المقياس المتوسط لنمذجة الخرسانة كمادة غير متجانسه تتكون من ماده ثلاثيه الطور (الركام الخشن, المونه و الفراغات الهوائية الموجودة في عجينة الاسمنت.الركام الخشن المستخدم لصب الاعتاب هو ركام مدور وركام مكسر وبمقاس اقصى 20 ملم. مقاومة الانضغاط لهذه الاعتاب هي 17 و 34 ميكاباسكال بالتعاقب. تم تصميم هذه الاعتاب الخرسانية المسلحة لتفشل نتيجه الانحناء عند تعرضها للتحميل النقطي على شكل (Two Point Load). هذه الاعتاب الخرسانية المسلحة تم دراستها مختبريا بالاضافه الى الدراسه العدديه. لنمذجة الركام الخشن بشكل واقعي ، يجب توزيع الركام بشكل عشوائي وفقًا للتدرج والكمية المستخدمة فعليًا في تصميم الخلطه. لعدم وجود هذه الخاصية في برنامج ABAQUS أدى إلى استخدام برنامج بديل لتمثيل الركام بشكل عشوائي. بعد ذلك ، ننقل التمثيل العشوائي للركام إلى برنامج ABAQUS باستخدام الأوامر والإرشادات التي يمكن فهمها من قبل البرنامج ، يتمكن من لرسمها كمخطط.

الكلمات الرئيسية –طريقة العناصر المحددة الممتدة، ميكانيك الانكسار، النمذجة المتوسطة المدى، تطور الشقوق.